

HOSTED BY



ELSEVIER

Available online at [www.sciencedirect.com](http://www.sciencedirect.com)

ScienceDirect

journal homepage: <http://ees.elsevier.com/ajps/default.asp>

## Original Research Paper

# Improved dissolution and bioavailability of silymarin delivered by a solid dispersion prepared using supercritical fluids

Gang Yang<sup>a</sup>, Yaping Zhao<sup>b</sup>, Nianping Feng<sup>a,\*</sup>, Yongtai Zhang<sup>a</sup>, Ying Liu<sup>a</sup>, Beilei Dang<sup>a</sup><sup>a</sup> School of Pharmacy, Shanghai University of Traditional Chinese Medicine, Shanghai 201203, China<sup>b</sup> School of Chemistry and Chemical Engineering, Shanghai Jiao Tong University, Shanghai 200240, China

## ARTICLE INFO

## Article history:

Received 8 October 2014

Received in revised form

8 December 2014

Accepted 13 December 2014

Available online 26 December 2014

## Keywords:

Silymarin

Solution-enhanced dispersion by supercritical fluids

Solid dispersion

Dissolution

Bioavailability

## ABSTRACT

The objective of this study was to improve the dissolution and bioavailability of silymarin (SM). Solid dispersions (SDs) were prepared using solution-enhanced dispersion by supercritical fluids (SEDS) and evaluated *in vitro* and *in vivo*, compared with pure SM powder. The particle sizes, stability, and contents of residual solvent of the prepared SM-SDs with SEDS and solvent evaporation (SE) were investigated. Four polymer matrix materials were evaluated for the preparation of SM-SD-SEDS, and the hydrophilic polymer, polyvinyl pyrrolidone K17, was selected with a ratio of 1:5 between SM and the polymer. Physicochemical analyses using X-ray diffraction and differential scanning calorimetry indicated that SM was dispersed in SD in an amorphous state. The optimized SM-SD-SEDS showed no loss of SM after storage for 6 months and negligible residual solvent (ethanol) was detected using gas chromatography. *In vitro* drug release was increased from the SM-SD-SEDS, as compared with pure SM powder or SM-SD-SE. *In vivo*, the area under the rat plasma SM concentration-time curve and the maximum plasma SM concentration were 2.4-fold and 1.9-fold higher, respectively, after oral administration of SM-SD-SEDS as compared with an aqueous SM suspension. These results illustrated the potential of using SEDS to prepare SM-SD, further improving the biopharmaceutical properties of this compound.

© 2014 Shenyang Pharmaceutical University. Production and hosting by Elsevier B.V. This is an open access article under the CC BY-NC-ND license (<http://creativecommons.org/licenses/by-nc-nd/4.0/>).

Abbreviations: HPMC, hydroxypropyl methylcellulose; PVP, polyvinyl pyrrolidone; SD, solid dispersion; SE, solution evaporation; SEDS, solution-enhanced dispersion by supercritical fluids; SM, silymarin.

\* Corresponding author. School of Pharmacy, Shanghai University of Traditional Chinese Medicine, No. 1200, Cailun Road, Shanghai 201203, China. Tel./fax: +86 21 51322198.

E-mail addresses: [npfeng@hotmail.com](mailto:npfeng@hotmail.com), [npfeng@shutcm.edu.cn](mailto:npfeng@shutcm.edu.cn) (N. Feng).

Peer review under responsibility of Shenyang Pharmaceutical University.

<http://dx.doi.org/10.1016/j.ajps.2014.12.001>

1818-0876/© 2014 Shenyang Pharmaceutical University. Production and hosting by Elsevier B.V. This is an open access article under the CC BY-NC-ND license (<http://creativecommons.org/licenses/by-nc-nd/4.0/>).

## 1. Introduction

Silymarin (SM), an extract of *Silybum marianum* (L.), contains a mixture of four flavonolignan isomers: silibinin (70–80%), silycristin (20%), silydianin (10%), and isosilybin (0.5%) [1,2]. Silybin is therefore the major component of SM and is responsible for its pharmacological activity. SM has traditionally been self-administered for the treatment of liver disorders [3,4]. The effects of SM on the liver have been attributed to its inhibition of hepatotoxin binding to receptor sites on the hepatocyte membrane; inhibition of glutathione oxidation, increasing its levels in the liver and intestine; antioxidant activity; and stimulation of ribosomal RNA polymerase and subsequent protein synthesis, leading to enhanced hepatocyte regeneration [5]. However, the effectiveness of SM as a liver disease remedy is limited by its poor aqueous solubility, resulting in low oral bioavailability due to poor enteral absorption [6]. Recently, various vehicles have been employed to improve the solubility and bioavailability of SM, such as solid lipid nanoparticles, microemulsion systems, liposomes, and solid dispersions (SDs) [7–10].

SDs have been used widely to enhance the dissolution rate of drugs with low aqueous solubility. In SD systems, a drug may exist as an amorphous form within a polymeric carrier. This may result in an increased drug dissolution rate, as compared with its crystalline form. The mechanisms involved in this SD-mediated enhancement of drug dissolution have been proposed by several investigators [11,12].

SDs can be prepared using a range of methods, such as melting, solvent evaporation, solvent melting, spray-drying, and supercritical fluid techniques. Supercritical fluid approaches have several advantages over more conventional preparation methods, including the ability to reduce residual organic solvent levels and to produce SDs with smaller particle sizes and better flowability [13]. There are several variants of supercritical fluid techniques, including rapid expansion of supercritical solutions, particles from gas-saturated solutions, gas antisolvent process, supercritical anti-solvent process, precipitation from compressed anti-solvent, aerosol solvent extraction system, and solution-enhanced dispersion by supercritical fluids (SEDS). SEDS provides the most promising method for the preparation of SD [14]. It uses semi-continuous processes to atomize the solution into a supercritical atmosphere. Provided that the drug is sparingly soluble in the supercritical fluid, which is highly soluble in the solvent, the supercritical fluid in the solvent droplets can produce an antisolvent effect. This process produces super-saturated solutions, facilitating precipitation of the solid in the form of small particles [15].

In the current study, SEDS was used to establish an SD delivery system for oral administration of SM, with the aim of enhancing drug dissolution and bioavailability. The physicochemical properties of SD prepared using several polymer materials were investigated, including polyvinyl pyrrolidone (PVP) K17, PVP K30, hydroxypropyl methylcellulose (HPMC) K4M, and HPMC K15M. In addition, analyses of stability and residual solvent were performed to compare SM-SD prepared by SEDS and by solvent evaporation (SE). *In vitro* dissolution and *in vivo* pharmacokinetics were analyzed to assess the SM-SD-SEDS.

## 2. Materials and methods

### 2.1. Materials

SM (purity >80%) and PVP K17 were purchased from Dalian Meilun Biotech Co., Ltd. (Dalian, China). PVP K30 was obtained from Sinopharm Chemical Reagent Co., Ltd. (Shanghai, China). HPMC K4M and HPMC K15M were supplied from Colorcon (USA). Carbon dioxide (CO<sub>2</sub>) with a purity of 99.99% was obtained from Shanghai Jiao Tong University (Shanghai, China). All other chemicals were reagent grade and used as received.

### 2.2. Animals

Animal studies of male Wistar rats weighing  $250 \pm 10$  g were conducted with the approval of the Animal Ethical Committee, Shanghai University of Traditional Chinese Medicine. The animals were kept in an agreeable environment with free access to a rodent diet and water and were acclimatized for at least 1 week before the start of the study.

### 2.3. Preparation of SM-SD

The supercritical pilot plant at Nantong Huaxing Petroleum Devices Co., Ltd. (Nantong, China), shown in a schematic diagram in Fig. 1A, was employed in this study. Briefly, this apparatus included three major components: a CO<sub>2</sub> delivery system, an organic solution delivery system, and a precipitation system. The supercritical CO<sub>2</sub> and the organic solution were separately pumped into the high pressure vessel through different inlets of the coaxial nozzle (the diameter of inner tubule was 0.2 mm and diameter of outside part was 1 mm) and continuously discharged from the bottom. The inner structure of the nozzle is shown in Fig. 1B. For preparation of SM-SD, CO<sub>2</sub> from the cylinder (Fig. 1A, 1) was refrigerated (2) and compressed to 15 MPa by the high-pressure pump (3) before the temperature controlling system (6) was activated to increase the temperature to 50 °C. The pressure of the precipitation system was increased by injection of CO<sub>2</sub> until the pressure reached 15 MPa. After the pressure and temperature of the view vessel (9) reached the required values, valve C was adjusted to maintain constant pressure in the vessel. Then SM and the excipients with the weight ratio of 1:5 (based on the results of preliminary experiment) were separately dissolved or dispersed in ethanol and a mixture of dichloromethane and ethanol (3/2, v/v). The solution was aspirated by a high pressure constant flow pump (11) (LC100, Nantong, China) at a flow rate of 1 ml/min. Supercritical CO<sub>2</sub> and the organic solution mixed and diffused rapidly. Solutes originally dissolved in the organic solvent rapidly reached super-saturation, resulting in the precipitation of SM-SD-SEDS in the vessel. Once the solution was exhausted, valve B was closed, and supercritical CO<sub>2</sub> was continuously pumped for about 40 min in order to remove residual organic solvent from the SM-SD. After that, valve A was closed while valve C remained open. The pressure of the precipitation vessel was slowly reduced and the product in the vessel was collected for further use.

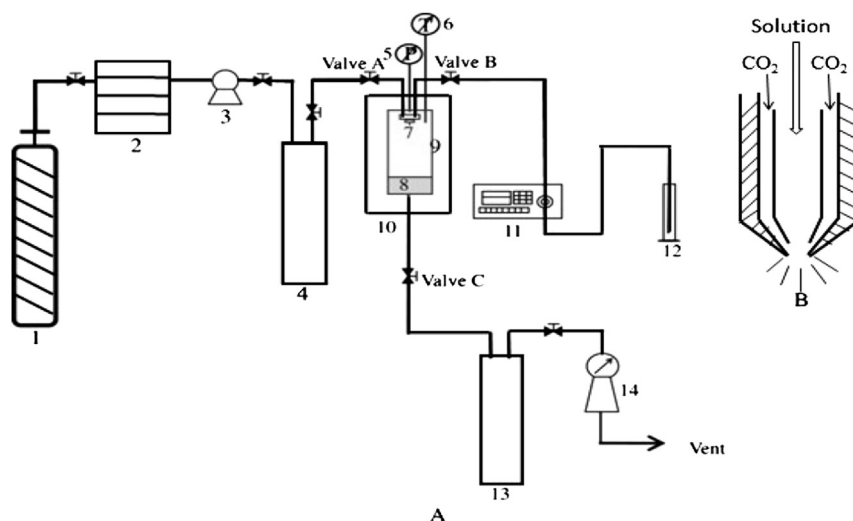


**Fig. 1** – Schematic diagram of the apparatus used for solution-enhanced dispersion by supercritical fluids. (A) (1) CO<sub>2</sub> cylinder, (2) refrigerator, (3) high-pressure pump, (4) stabilization tank, (5) pressure sensor, (6) temperature sensor, (7) nozzle, (8) filter, (9) view vessel, (10) air bath, (11) high pressure constant flow pump, (12) graduated flask, (13) separator, (14) wet gas meter. (B) The structure of the nozzle.

SM-SDs were also prepared using the SE method, whereby the drug and matrix were both dissolved in ethanol, and the solvent was removed under vacuum in a rotary evaporator (R-205, Shanghai, China). The resultant SM-SD-SE was placed in a vacuum drying oven (DHG-9070A, Shanghai, China) to harden prior to pulverization, sieving through a 250- $\mu$ m sieve, and storage in a desiccator.

#### 2.4. High-performance liquid chromatography (HPLC) analysis

The content of SM was determined using an HPLC system (LC-2010A HT, Shimadzu, Japan) with an Agilent Eclipse XDB-C18 column (5  $\mu$ m, 4.6  $\times$  250 mm) (Agilent, Shanghai, China). The mobile phase consisted of methanol and pure water (46:54, v/v) at a flow rate of 0.8 ml/min. The effluent was monitored at 288 nm.

#### 2.5. In vitro dissolution

The rate of dissolution of SM from the indicated preparations was evaluated using the small vessel method. The dissolution medium was phosphate buffer solution (pH 6.8) containing 0.3% (w/v) sodium dodecyl sulfate and maintained at  $37 \pm 0.5$  °C stirring at 100 rpm. Samples of 2.0 ml were withdrawn after 5, 10, 15, 20, 30, 60, 90, 120 min, and replaced by the same volume of fresh medium at  $37 \pm 0.5$  °C. The samples were filtered through a 0.45- $\mu$ m membrane, and the SM content was determined by HPLC, as described in Section 2.4. Each experiment was carried out in triplicate.

#### 2.6. Scanning electron microscopy (SEM)

The SD surface morphology was observed by SEM (NOVA NanoSEM 250, Shanghai, China). Samples were sprayed with

gold before examination. Microphotographs were obtained using an accelerating voltage of 5 kV at 1000–25,000  $\times$  magnification.

#### 2.7. X-ray diffraction (XRD)

Samples were analyzed using an X-ray polycrystalline diffractometer (D8 ADVANCE, Bruker, Germany). Cu K $\alpha$  radiation was used as the X-ray source. Samples were scanned over the range of 50°–70° 2 $\theta$  at a scanning speed of 6°/min and a step size of 0.02°. The voltage was set at 40 kV and the current was 40 mA.

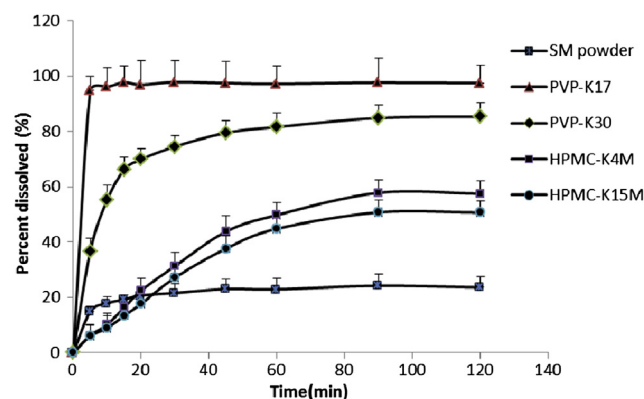


**Fig. 2** – In vitro dissolution profiles. The cumulative release of silymarin (SM) in phosphate buffer solution (pH = 6.8) is shown from SM powder and SM solid dispersions (SDs) prepared by solution-enhanced dispersion by supercritical fluids (SEDS) using the indicated carriers ( $n = 3$ ). PVP, polyvinyl pyrrolidone; HPMC, hydroxypropyl methylcellulose.

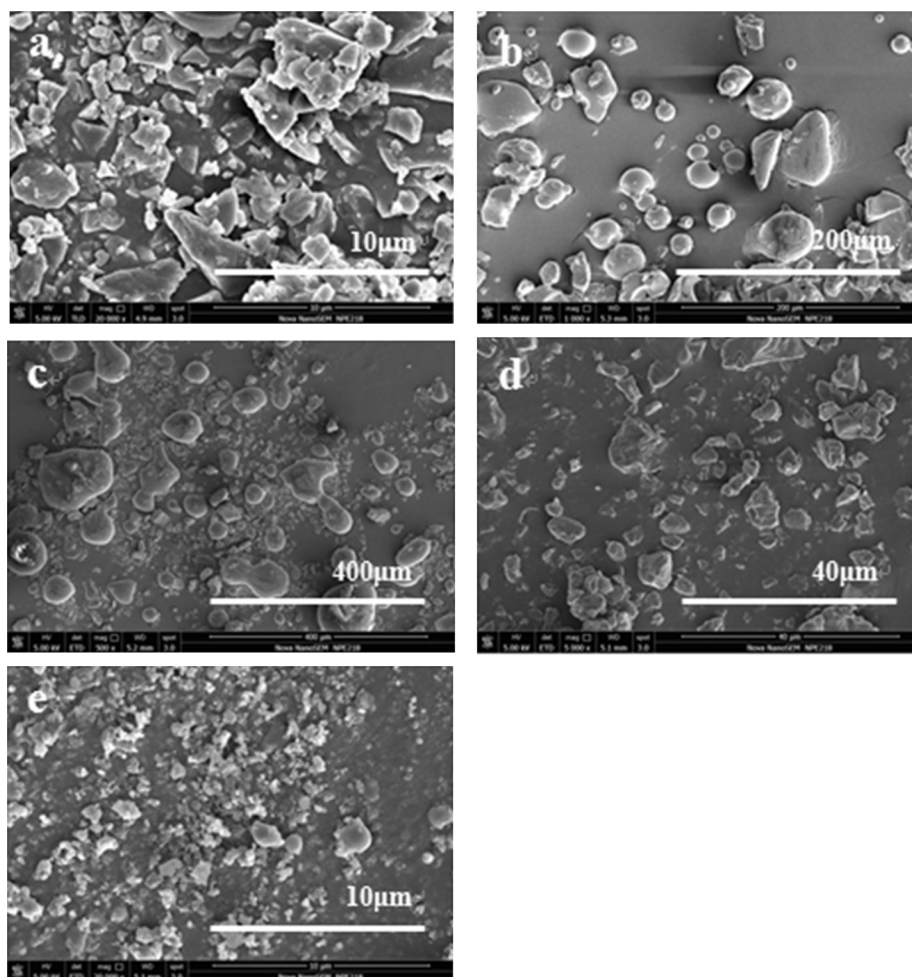


**Fig. 3 – Scanning electron microscopy images. (a) Silymarin (SM) powder, (b) polyvinyl pyrrolidone (PVP) K17, (c) physical mixture of SM and PVP K17, (d) SM solid dispersion (SD) generated using solvent evaporation, (e) SM-SD generated using solution-enhanced dispersion by supercritical fluids.**

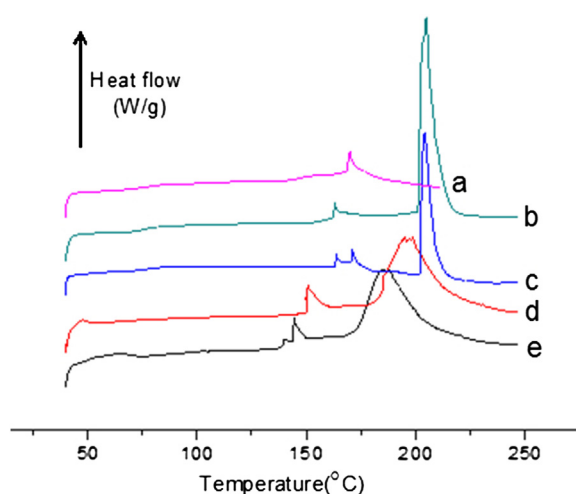


**Fig. 4 – Differential scanning calorimetry analyses. (a) Silymarin (SM) powder, (b) polyvinyl pyrrolidone (PVP) K17, (c) physical mixture of SM and PVP K17, (d) SM solid dispersion (SD) generated using solution-enhanced dispersion by supercritical fluids, (e) SM-SD generated using solvent evaporation.**

## 2.8. Differential scanning calorimetry (DSC)

The thermal behaviors of the SD samples were analyzed using a differential scanning calorimeter (Q2000, New Castle, USA). SD (~5–10 mg) was sealed in a specialized aluminum pan using an aluminum lid with a pinhole. Measurements were performed over 40–250 °C under a dry nitrogen atmosphere at a heating rate of 10 °C/min.

## 2.9. Stability studies

The SM content of the SM-SD preparations was analyzed at 0, 1, 2, 4, and 6 months to compare the degradation over time, and XRD was used to investigate the physical stability of SM-SD.

## 2.10. Determination of residual solvent

The ethanol content of the SM-SD preparations was analyzed by gas chromatography to monitor the efficiency of solvent removal during SEDS. The samples were dissolved in acetone.

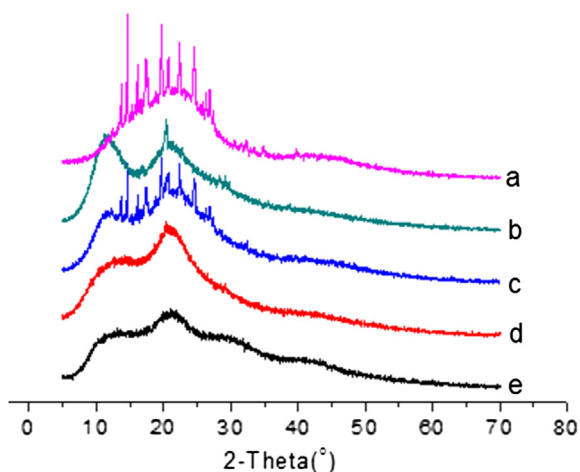


Fig. 5 – X-ray diffraction analyses. (a) silymarin (SM) powder, (b) polyvinyl pyrrolidone (PVP) K17, (c) physical mixture of SM and PVP K17, (d) SM solid dispersion (SD) generated using solution-enhanced dispersion by supercritical fluids, (e) SM-SD generated using solvent evaporation.

Table 1 – The silymarin (SM) content of the indicated preparations after storage at room temperature for the indicated time periods (as a percentage of the level at 0 month).

Months	SM powder (%)	SM-SD-SEDS (%)	SM-SD-SE (%)
1	99.92	99.13	97.79
2	99.86	98.67	95.61
4	99.64	96.41	92.34
6	99.57	95.25	90.18

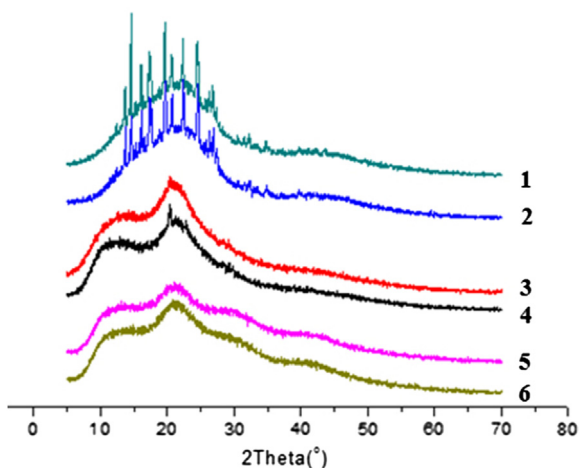


Fig. 6 – X-ray diffraction analyses. Silymarin (SM) powder was analyzed on day 0 (1) and after 6 months (2); SM solid dispersion (SD) generated using solvent evaporation on day 0 (3) and after 6 months (4); and SM-SD generated using solution-enhanced dispersion by supercritical fluids at day 0 (5) and after 6 months (6).

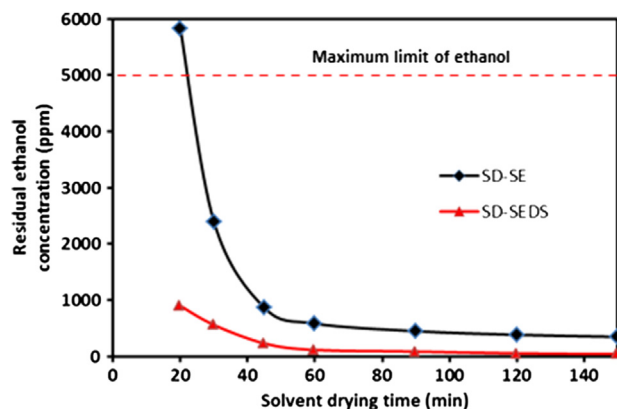


Fig. 7 – The concentration of residual ethanol in solid dispersions (SD). The levels of ethanol are shown in SDs prepared by solution-enhanced dispersion by supercritical fluids (SEDS) and solvent evaporation (SE).

An Agilent 7890A gas chromatography system coupled with a flame ionization detector (Agilent, California, USA) and an Agilent 19091N-113 HP-INNOWAX capillary column (30 m × 0.32 mm × 0.25 μm, Agilent, California, USA) was employed, using nitrogen as the carrier gas. The 20:1 split mode was used, while the injection port was operated at 150 °C. The initial oven temperature was held at 50 °C for 10 min, and then raised to 200 °C for 10 min at a heating rate of 5 °C/min. The temperature of hydrogen flame ionization detector was set at 250 °C.

### 2.11. *In vivo* pharmacokinetics

Male Wistar rats (Section 2.2) were randomly divided into two groups ( $n = 6$ /group). The animals were starved for 12 h before the experiment but had free access to water. One group of rats was orally administered 20 mg/kg SM, contained within

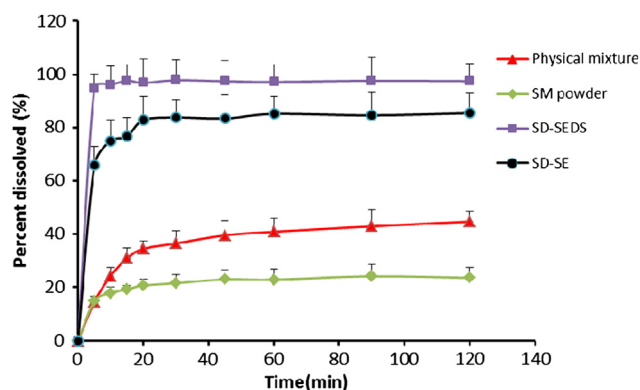
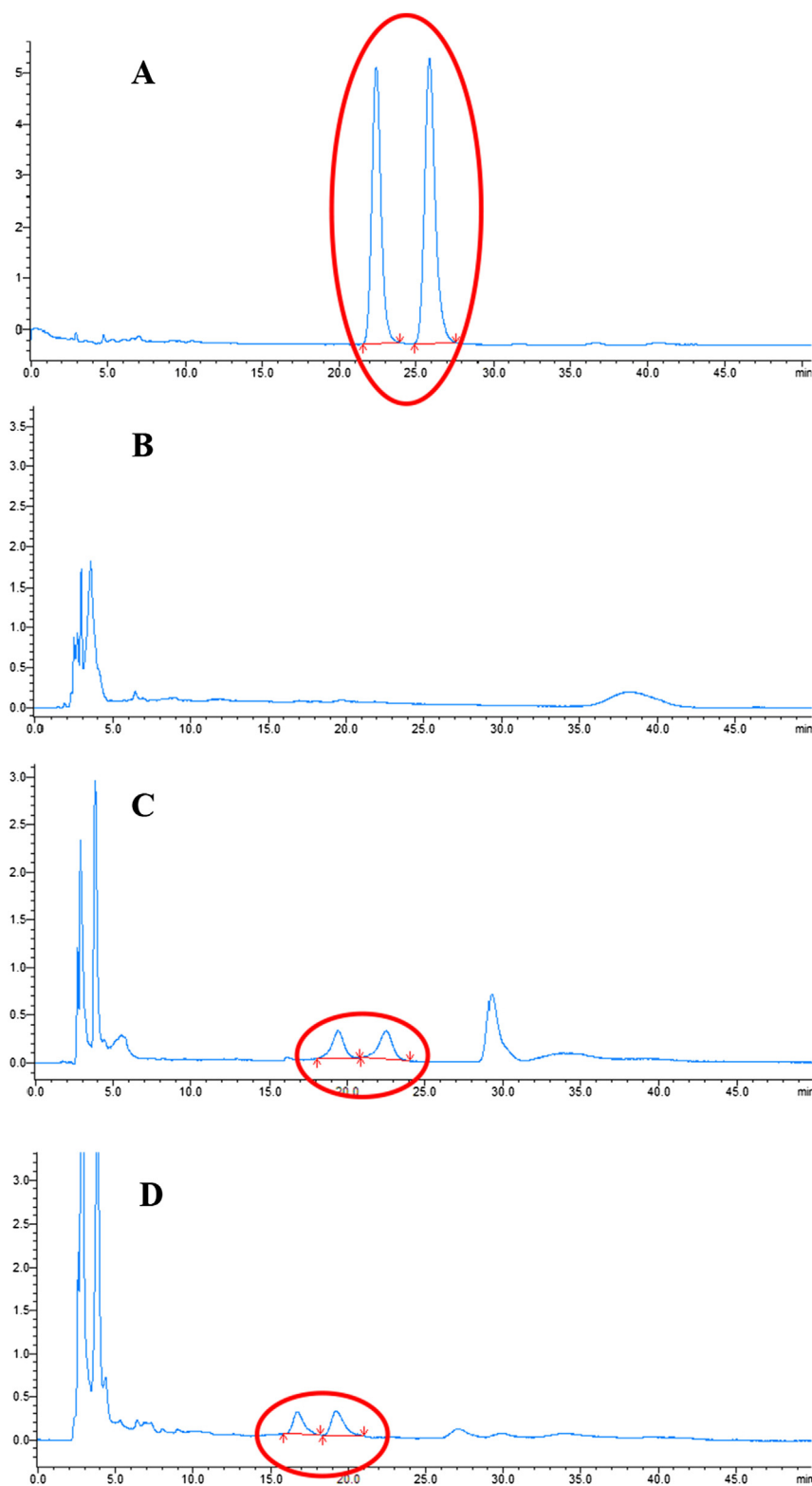


Fig. 8 – *In vitro* release of silymarin (SM) in phosphate buffer solution (pH = 6.8). The cumulative release of SM is shown from SM powder, a physical mixture of SM and polyvinyl pyrrolidone (PVP) K17, SM solid dispersion generated using solvent evaporation (SM-SD-SE), and SM solid dispersion generated using solution-enhanced dispersion by supercritical fluids (SM-SD-SEDS) ( $n = 3$ ).

SM-SD-SEDS, and the second group of rats received an aqueous suspension of SM (prepared by simply adding SM to purified water). About 0.3-ml blood samples were collected from the eye socket vein and placed in heparinized tubes at

the indicated time points after dosing. The blood samples were centrifuged (Eppendorf, Hamburg, Germany) at 5000 rpm for 10 min to isolate the plasma. One milliliter of ethyl acetate was added to the plasma and vortex-mixed (IKA, Staufen,



**Fig. 9** – High-performance liquid chromatography determination of silymarin (SM). Typical SM chromatograms for: (A) silybin; (B) blank Wistar rat plasma; (C) Wistar rat plasma spiked with silybin; (D) Wistar rat plasma after oral administration of SM solid dispersion generated using solution-enhanced dispersion by supercritical fluids (SM-SD-SEDS).

Germany) for 1 min, and then centrifuged at 10,000 rpm for 10 min. The supernatant layer was dried under nitrogen and redissolved in 100  $\mu$ l methanol prior to HPLC determination, as described in Section 2.4.

### 2.12. Statistical analysis

All the generated data were presented as mean  $\pm$  standard deviation. The pharmacokinetic parameters were estimated by a non-compartmental model using DAS 2.0 software. Statistical analyses were conducted by one-way analysis of variance (ANOVA). A value of  $P < 0.05$  was considered statistically significant.

## 3. Results and discussion

### 3.1. In vitro SM release from SD prepared using various polymeric matrices

In this study, SM-SDs were successfully prepared by SEDS using each of the following excipients; PVP K17, PVP K30, HPMC K4M, and HPMC K15M. The cumulative release of SM from the formulated SDs (Fig. 2) was markedly improved as compared with SM powder. There were significant differences between the samples in terms of their *in vitro* SM release (ANOVA,  $P < 0.05$ ). The PVP K17-based SD showed the most effective SM release over the test period, achieving 98% cumulative drug release in 15 min. These results demonstrated that the SDs improved SM dissolution, as compared with the raw drug powder, in the following order: SM powder < HPMC K15M < HPMC K4M < PVP K30 < PVP K17. As previously reported, PVP K17 forms reticulate structures and incorporation of drug molecules into these results in molecular dispersion [16], which may contribute to increased drug dissolution and release.

### 3.2. SEM

Fig. 3 shows SEM images of SM powder, PVP K17, a physical mixture of SM and PVP K17, and SM-SD generated by SE or SEDS. The physical mixture of SM and PVP K17 had a different morphology to that of SM-SD-SE and SM-SD-SEDS, with the SM-SD-SEDS showing the smaller size distribution; this may contribute to enhanced drug solubility.

### 3.3. DSC

Sample DSC curves are shown in Fig. 4. For SM powder, a sharp endothermic peak was observed at 169.98  $^{\circ}$ C, corresponding to its melting point. The melting endotherm for PVP K17 was observed at 204.82  $^{\circ}$ C. The DSC analysis showed no relocation of peaks in the physical mixture, where the characteristic melting points of PVP K17 and SM remained unchanged. This indicated that there were no chemical drug–polymer interactions. However, the endothermic peak of SM was not observed in SDs prepared by SEDS and SE, and the endothermic peak of PVP K17 had shifted. These results suggested that SM was present in a different state in the SM-SD.

### 3.4. XRD

To examine crystal morphology, XRD analyses were carried out and the patterns generated by SM, PVP K17, the physical mixture of PVP K17 and SM, and SM-SD prepared by SEDS and SE were presented in Fig. 5. SM powder showed a crystalline structure, as demonstrated by its sharp and intense diffraction peaks. These diffraction peaks were retained in the physical mixture, suggesting that SM remained in a crystalline state. In contrast, these characteristic peaks were absent in SM-SDs, indicating that SM was in an amorphous state. These XRD results were in agreement with the DSC results. The amorphous state of SM within SDs may contribute to increased drug solubility [17,18].

### 3.5. Stability

SDs have been demonstrated to be effective formulations for the improvement of drug solubility, but they may have a critical drawback in terms of stability. The recrystallization of amorphous drugs in SD may lead to a reduced dissolution rate and consequently a lower bioavailability [19,20]. The data generated by SM content analysis and XRD of SM-SD were presented in Table 1 and Fig. 6. The SM content of SM powder and SM-SD produced by SEDS or SE was not significantly changed following storage for six months. However, more drug loss was observed in SM-SD-SE than in SM-SD-SEDS. This may reflect increased molecular motion within SM-SD-SE, recrystallization of the amorphous drug, and the associated chemical degradation [21,22]. Furthermore, the XRD result for SM-SD-SEDS was similar on day 0 and at 6 months (Fig. 6), indicating that the drug remained in an amorphous state throughout the test period. However, the profile from SM-SD-SE showed a sharp peak at 21 $^{\circ}$  2 $\theta$ , which could suggest a certain degree of drug recrystallization in this formulation. Previous reports have indicated that residual solvent in SDs could promote nucleation for crystallization and thereby

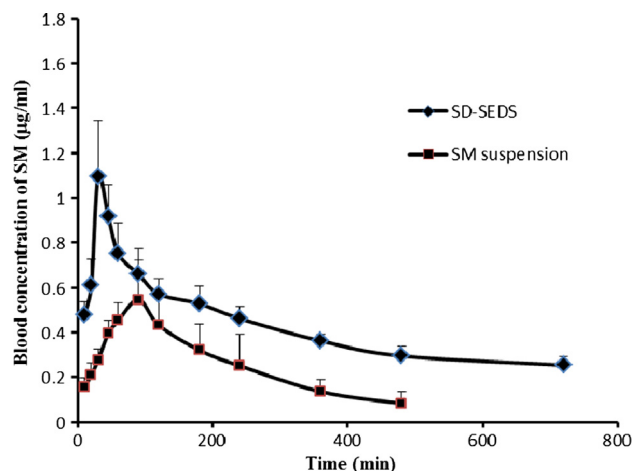


**Fig. 10 – In vivo plasma concentration-time profiles. Levels of silymarin (SM) following oral administration of the SM solid dispersion generated using solution-enhanced dispersion by supercritical fluids (SM-SD-SEDS) or aqueous SM suspension ( $n = 6$ ).**

**Table 2 – The main pharmacokinetic parameters of the indicated preparations in male Wistar rats (n = 6).**

Formulation	$T_{\max}$ (h)	$C_{\max}$ ( $\mu\text{g/ml}$ )	$\text{AUC}_{0-t}$ ( $\mu\text{g/ml}\cdot\text{h}$ )	$t_{1/2}$ (h)
SM powder	$1.45 \pm 0.447$	$0.57 \pm 0.143$	$2.054 \pm 0.074$	$2.938 \pm 0.694$
SM-SD-SEDS	$0.5 \pm 0.13$	$1.093 \pm 0.249$	$5.017 \pm 0.358$	$7.830 \pm 3.204$

promote degradation of the active ingredients. This may therefore have contributed to the greater drug loss and the altered XRD of SM-SD-SE, as compared with SM-SD-SEDS.

### 3.6. Residual solvent

The solvent remaining in SD after the preparation progress can affect drug stability and is also potentially harmful to public health, depending on the solvent(s) employed [23,24]. The residual ethanol was measured in the SM-SD prepared in the present study and the results were shown in Fig. 7. The presence of a certain amount of ethanol (5000 ppm) is considered acceptable without justification in pharmaceuticals. In SM-SD-SE, residual ethanol was reduced from a level of approximately 6000 ppm (after being dried for 20 min with rotary evaporation) to about 300 ppm after being dried for 140 min (Fig. 7). However, the residue ethanol level was much lower in SM-SD-SEDS, at approximately 1000 ppm after the initial 20-min drying period, and almost no residual ethanol after 140 min. These results indicated that more residual solvent was removed from SD generated using SEDS, rather than SE.

### 3.7. In vitro dissolution test

The dissolution profiles shown in Fig. 8 indicated that SM-SD exhibited faster drug release than the other preparations tested. As previously reported, rapid hydration of hydrophilic polymers promotes the drug wetting process in aqueous surroundings and enlarges the surface area of the solid–water interface, which may contribute to the improved SD dissolution rate [25]. However, SM-SD-SEDS showed a cumulative release of more than 90% in the first 5 min, whereas less than 70% release was observed from SM-SD-SE at 5 min. This may be due to the decreased particle size and reduced surface tension of the dissolution medium [26] when using supercritical fluid technology.

### 3.8. Pharmacokinetics

Plasma SM was completely separated under the analytical conditions employed in this study. Silybin is an isomeric compound and two peaks were detected at about 18 and 21 min. The sum of the area of the two peaks was used for these pharmacokinetic analyses (Fig. 9). Standard curves were linear ( $r = 0.9996$ ) over the range of  $0.08\text{--}3\ \mu\text{g/ml}$ . The results obtained using this method indicated recoveries of  $96.43 \pm 1.43\%$ ,  $97.75 \pm 1.04\%$ , and  $97.93 \pm 1.46\%$  at low, middle, and high concentrations, respectively. The detection limit was  $30\ \text{ng/ml}$ .

Rat plasma SM was quantified in vivo after oral administration of an aqueous suspension of SM or SM-SD-SEDS. These plasma profiles were compared in Fig. 10. The plasma SM concentration following administration of SM-SD-SEDS indicated more effective drug absorption, as compared with the

SM aqueous suspension. All pharmacokinetic parameters (maximum plasma concentration [ $C_{\max}$ ], time of  $C_{\max}$  [ $T_{\max}$ ], area under the plasma concentration–time curve [ $\text{AUC}_{0-t}$ ], and plasma half-life [ $t_{1/2}$ ]) were calculated individually for each subject in the group and the values were expressed as mean  $\pm$  standard deviation ( $n = 6$ ) (Table 2).

The  $\text{AUC}_{0-t}$  of SM-SD-SEDS was 2.4-fold larger than that of SM suspension and this difference was statistically significant ( $P < 0.01$ ).  $C_{\max}$  was also 1.9-fold higher and  $T_{\max}$  occurred earlier after oral administration of SM-SD-SEDS, as compared with SM aqueous suspension. These findings indicated that SM-SD prepared by SEDS could provide a promising strategy for improving the bioavailability of SM. The enhanced bioavailability of SM delivered by SDs could be attributed to their improved rate of dissolution, which would facilitate drug absorption [27].

## 4. Conclusions

In summary, SM-SDs were successfully prepared using SEDS. The resultant SM-SD-SEDS considerably improved the drug dissolution profile and increased its oral absorption, as compared with SM powder. This study was innovative in its application of a new, high-efficiency, and environmentally-friendly method to produce SDs and improve the dissolution and bioavailability for drugs with low aqueous solubility. Although future studies will be required to increase the oral bioavailability of SM further, the present study proved that supercritical fluid technology provided a viable alternative means to prepare drug-loaded SDs.

## Acknowledgments

This work was supported financially by the Subject Chief Scientist Program (10XD14303900) from Science and Technology Commission of Shanghai Municipality, and the Specialized Research Fund for the Doctoral Program of Higher Education of China (20123107110005).

## REFERENCES

- [1] Luper S. A review of plants used in the treatment of liver diseases: part 1. *Altern Med Rev* 1998;3:410–421.
- [2] Pradhan SC, Girish C. Hepatoprotective herbal drug, silymarin from experimental pharmacology to clinical medicine. *Indian J Med Res* 2006;124:491–504.
- [3] Mohamed ES, Gamal ES, Tarek MI. Comparison of early treatment with low doses of nilotinib, imatinib and a clinically relevant dose of silymarin in thioacetamide-induced liver fibrosis. *Eur J Pharmacol* 2001;670:593–600.



- [4] Freedman ND, Curto TM, Morishima C. Silymarin use and liver disease progression in the hepatitis C antiviral long-term treatment against cirrhosis trial. *Aliment Pharm Ther* 2010;33:127–137.
- [5] Dixit N, Baboota S, Kohli K, et al. Silymarin: a review of pharmacological aspects and bioavailability enhancement approaches. *Indian J Pharmacol* 2007;39:171–179.
- [6] Giacomelli S, Gallo D, Apollonio P, et al. Silybin and its bioavailable phospholipid complex (IdB1016) potentiate *in-vitro* and *in-vivo* activity of cisplatin. *Life Sci* 2003;70:1447–1459.
- [7] Shangguan MZ, Yi Lu, Qi JP, et al. Binary lipids-based nanostructured lipid carriers for improved oral bioavailability of silymarin. *J Biomater Appl* 2014;28:887–896.
- [8] Panapisal V, Charoensri S, Tantituvanont A. Formulation of microemulsion systems for dermal delivery of silymarin. *PharmSciTech* 2012;13:389–399.
- [9] Ahmed S, Mohammed E, Mohammad A. Complement activation assay and *in vivo* evaluation of silymarin loaded liver targeting liposome. *J Life Med* 2014;2:15–24.
- [10] Sonali D, Tejal S, Vaishali T, et al. Silymarin-solid dispersions: characterization and influence of preparation methods on dissolution. *Acta Pharm* 2010;60:427–443.
- [11] Bobe K, Bobe CR, Suresh S. Formulation and evaluation of solid dispersion of atorvastatin with various carriers. *Pharmacie Globale (IJCP)* 2011;1:1–6.
- [12] Das SK, Roy S, Kalimuthu Y. Solid dispersions: an approach to enhance the bioavailability of poorly water-soluble drugs. *Int J Pharmacol Pharm Technol* 2014;1:2277–3436.
- [13] Won DH, Kim MS, Lee S, et al. Improved physicochemical characteristics of felodipine solid dispersion particles by supercritical anti-solvent precipitation process. *Int J Pharm* 2005;301:199–208.
- [14] Juppo AM, Boissier C, Khoo C. Evaluation of solid dispersion particles prepared with SEDS. *Int J Pharm* 2003;250:385–401.
- [15] Antonio T, Eva M, Miguel A. Precipitation of tretinoin and acetaminophen with solution enhanced dispersion by supercritical fluids (SEDS). *Powder Technol* 2012;217:177–188.
- [16] Chen ZQ, Liu Y, Zhao JH, et al. Improved oral bioavailability of poorly water-soluble indirubin by a supersaturatable self-microemulsifying drug delivery system. *Int J Nanomedicine* 2012;7:1115–1125.
- [17] Kim MS, Jin SJ, Kim JS. Preparation, characterization and *in vivo* evaluation of amorphous atorvastatin calcium nanoparticles using supercritical antisolvent (SAS) process. *Eur J Pharm Biopharm* 2008;69:454–465.
- [18] Juan J, Garcia R, Paloma M, et al. Changed crystallinity of mebendazole solid dispersion: improved anthelmintic activity. *Int J Pharm* 2011;403:23–28.
- [19] Han HK, Lee BJ, Lee HK. Enhanced dissolution and bioavailability of biochanin A via the preparation of solid dispersion: *in vitro* and *in vivo* evaluation. *Int J Pharm* 2011;415:89–94.
- [20] Guo YS, Shalaev E, Scott S. Physical stability of pharmaceutical formulations: solid-state characterization of amorphous dispersions. *TRAC-Trend Anal Chem* 2013;49:137–144.
- [21] Patrick JM, Alfred CFR, David EN, et al. Effect of temperature and moisture on the miscibility of amorphous dispersions of felodipine and poly (vinyl pyrrolidone). *J Pharm Sci* 2009;99:169–185.
- [22] Sarode AL, Sandhu H, Shah N, et al. Hot melt extrusion for amorphous solid dispersions: temperature and moisture activated drug-polymer interactions for enhanced stability. *Mol Pharmaceut* 2013;10:3665.
- [23] Deconinck E, Canfyn M, Sacre PY, et al. Evaluation of the residual solvent content of counterfeit tablets and capsules. *J Pharmaceut Biomed* 2013;81:80–88.
- [24] Ke K, Wei XF, Bao RY, et al. Contribution of residual solvent to the nucleation and reinforcement of poly (vinylidene fluoride). *Polym Test* 2014;34:78–84.
- [25] Park YJ, Xuan JJ, Oh DH, et al. Development of novel itraconazole-loaded solid dispersion without crystalline change with improved bioavailability. *Arch Pharm Res* 2010;33:1217–1225.
- [26] Park J, Cho W, Cha KH. Solubilization of the poorly water soluble drug, telmisartan, using supercritical anti-solvent (SAS) process. *Int J Pharm* 2013;441:50–55.
- [27] Li SM, Liu Y, Liu T, et al. Development and *in-vivo* assessment of the bioavailability of oridonin solid dispersions by the gas anti-solvent technique. *Int J Pharm* 2011;411:172–177.